Initial Results of Triton Burnup Study in the Large Helical Device*)

Neng PU[1)], Takeo NISHITANI[2)], Kunihiro OGAWA[1,2)], Mitsutaka ISOBE[1,2)], Sadayoshi MURAKAMI[3)] and LHD Experiment Group[2)]

[1)]*SOKENDAI (The Graduate University for Advanced Studies), Toki, Gifu 509-5292, Japan*
[2)]*National Institute for Fusion Science, National Institutes of Natural Sciences, Toki, Gifu 509-5292, Japan*
[3)]*Kyoto University, Kyoto 615-8540, Japan*

(Received 3 January 2018 / Accepted 5 October 2018)

The deuterium plasma experiments have been conducted since March 2017 on the Large Helical Device. The neutron yield per shot has reached up to 7×10^{14} and 3.5×10^{15} in the first phase where NBI #1, 2, and 3 used hydrogen and NBI #4 and 5 used deuterium, and in full D-D phase, respectively. For the triton burnup study in this campaign, the neutron activation system (NAS) has been used to measure 14 MeV neutrons and 2.45 MeV neutrons. The triton burnup ratio of 0 ~ 0.34% are obtained by the NAS measurement. Triton burnup ratio increases with electron density when line-averaged electron density is below about 2.5×10^{19} m^{-3}, and decreases with electron density above 2.5×10^{19} m^{-3}. Meanwhile, the triton burnup ratio decreases as the magnetic axis positions shift outward, which can likely be explained by the orbit of helically trapped energetic tritons. In addition to the NAS measurement, the phenomenon of the 14 MeV neutron emission lagging at the 2.45 MeV neutrons emission has been observed by the time evolution measurement with scintillating-fiber detectors and neutron flux monitor.

Keywords: triton burnup, LHD, neutron activation, 14 MeV neutron, alpha confinement

DOI: 10.1585/pfr.13.3402121

1. Introduction

The Large Helical Device (LHD) is a large superconducting heliotron device in Japan, having a major radius of 3.9 m and averaged plasma minor radius of ~ 0.6 m [1]. In the LHD, the deuterium plasma operation started in March 2017 to explore high-performance deuterium plasmas of LHD. The neutron yield measurement is essential for the LHD deuterium projects in terms of the radiation safety, the evaluation of the fusion output, and the study of the energetic-particle confinement. To evaluate the total neutron yield from LHD deuterium plasmas, a wide dynamic range neutron flux monitor (NFM) [2] and a neutron activation system (NAS) [3] are employed in LHD [4]. The NFM on LHD consists of three ^{235}U fission chambers and three high-sensitivity thermal neutron detectors, which placed on the top of LHD and outside equatorial port. NAS located on inside the equatorial port (8-O port) and the vertical port (2.5-L port) using indium (In) foil for 2.45 MeV neutron measurement and silicon (Si) foil for 14 MeV neutron measurement. The NFM plays a primary role in the evaluation of the total neutron yield. Although NAS does not provide time evolution of neutron emission rate, it is absolutely insensitive to gamma-rays and is of great value to perform cross check of the neutron yield evaluated by NFM [5, 6]. In the tokamaks such as TFTR [7], JET [8], ASDEX-U [9], JT-60U [10], DIII-D [11], FT [12], PLT [13], and KSTAR [14], neutron activation techniques have been applied to measure the neutron yield in the deuterium plasmas.

In deuterium plasmas, 2.45 MeV neutrons and 1 MeV tritons are produced with almost the same production rate. Energetic tritons will undergo secondary D-T reaction with background deuteron while those tritons slow down. If secondary 14 MeV neutrons can be measured selectively, we can study the confinement of 1 MeV tritons. Kinematic properties such as the Larmor radius and the precessional drift frequency of 1 MeV tritons are almost the same as those of 3.5 MeV alphas in D-T plasmas. Therefore, the triton burnup study is useful to estimate the behavior of D-T born alphas. The triton burnup study is one of the important physics subjects in the LHD deuterium project to demonstrate alpha particle confinement in the LHD-type magnetic field configuration. NAS plays an important role in the triton burnup study through measurements of secondary 14 MeV neutron yield. Meanwhile, in this campaign, two scintillating-fiber (Sci.-Fi.) detectors placed to close the outside 8-O port and just under the flange of 2.5-L port were used to measure the time evaluation of 14 MeV neutrons [15]. In the Sci.-Fi. detectors, about 100 scintillating fibers were embedded into aluminum matrix for stopping recoil proton and electron passing into adjacent fiber to reduce the contribution from low energy neutrons and gamma-rays. High pulses generated forwardly recoiled high-energy protons due to 14 MeV neutrons are

author's e-mail: pu.neng@nifs.ac.jp
*) This article is based on the presentation at the 26th International Toki Conference (ITC26).

picked up by discriminator.

2. Comparison of NAS, NFM and Sci.-Fi.

In situ calibration of NAS was performed by using ^{252}Cf source prior to the LHD first deuterium plasma campaign [3]. The neutron yield per shot has reached up to 7×10^{14} and 3.5×10^{15} in the first phase where NBI #1, 2, and 3 used hydrogen and NBI #4 and 5 used deuterium, and in full D-D phase, respectively. Shot-integrated neutron yields are evaluated in deuterium plasmas heated by perpendicular deuterium NBIs by using ^{115}In(n,n')$^{115\mathrm{m}}$In reaction with the results from in situ calibration experiment. Those results are utilized to perform cross checking of the absolute total neutron yield measured by NFM as shown in Fig. 1 (a). Relative deviations between the NAS and NFM are less than 10%. Red line in Fig. 1 (a) indicates that the total neutron yield evaluated by NAS is consistent with that measured by NFM. Meanwhile, 14 MeV neutron yield measured by Sci.-Fi. detector has been calibrated by 14 MeV neutron yield measured by NAS using ^{28}Si(n, p)^{28}Al reaction as shown in Fig. 1 (b). The relative deviations between NAS and Sci-Fi is 10% ~ 30%.

(a)

(b)

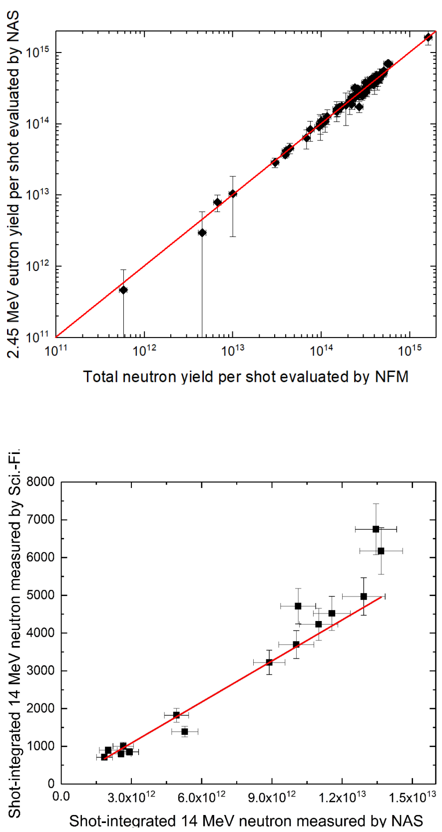

Fig. 1 (a) Comparison of 2.45 MeV neutron yield measured by NAS and total neutron yield measured by NFM, (b) comparison of 14 MeV neutron yield measured by NAS and 14 MeV neutron yield measured by Sci.-Fi. detector.

3. Parameter Dependence of Triton Burnup Ratio

Triton burnup ratio is defined as 14 MeV neutron yield divided by 2.45 MeV neutron yield as follows:

$$\text{Triton burnup ratio} = \frac{S_{\mathrm{DT}}}{S_{\mathrm{DD}}}, \tag{1}$$

where S_{DT} and S_{DD} are 14 MeV and 2.45 MeV neutron emission rates, respectively. S_{DT} is represented by

$$S_{\mathrm{DT}} = n_{\mathrm{D}} \cdot n_{\mathrm{T}} \cdot \langle \sigma v \rangle_{\mathrm{DT}}, \tag{2}$$

where n_{D} and n_{T} are the bulk deuteron ion density and the fast triton density, respectively, and $\langle \sigma v \rangle_{\mathrm{DT}}$ is the reactivity between bulk deuterons and fast tritons. If the fast triton loss is negligible,

$$n_{\mathrm{T}} = S_{\mathrm{Triton}} \cdot \tau_{\mathrm{se}} = S_{\mathrm{DD}} \cdot \tau_{\mathrm{se}}, \tag{3}$$

where S_{Triton} is triton birth rate, which is equal to S_{DD}. Therefore,

$$\begin{aligned} \text{Triton burnup ratio} &= n_{\mathrm{D}} \tau_{\mathrm{se}} \langle \sigma v \rangle_{\mathrm{DT}} \\ &\approx n_{\mathrm{e}} \tau_{\mathrm{se}} \langle \sigma v \rangle_{\mathrm{DT}}. \end{aligned} \tag{4}$$

Here, the slowing-down time τ_{se} is a function of temperature T_{e} and density n_{e}. The slowing-down time for triton can be written as follow [16].

$$\tau_{\mathrm{se}} = 8.21 \times 10^{7} \frac{(T_{\mathrm{e}})^{3/2}}{n_{\mathrm{e}}}. \tag{5}$$

If the loss of the fast triton is not negligible, EQ (4) is modified by

$$\text{Triton burnup ratio} \approx n_{\mathrm{e}} \tau_{\mathrm{eff}} \langle \sigma v \rangle_{\mathrm{DT}}, \tag{6}$$

where,

$$\frac{1}{\tau_{\mathrm{eff}}} = \frac{1}{\tau_{\mathrm{c}}} + \frac{1}{\tau_{\mathrm{se}}}. \tag{7}$$

Here, τ_{c} is the confinement time of fast ions, and τ_{eff} is the effective confinement time of fast ions.

In the LHD first deuterium plasma campaign, 14 MeV neutrons and 2.45 MeV neutrons have been measured by NAS for the triton burnup study. The triton burnup ratio was measured with NAS to be 0 ~ 0.34% in the magnetic axis position of 3.6 m and magnetic field strength of 2.75 T. The NAS measurements indicate that the triton burnup ratio increases with $\overline{n_{\mathrm{e}}}$ below about $2.5 \times 10^{19}\ \mathrm{m}^{-3}$, and decreases from that density. In the low-n_{e} phase, τ_{se} is long, thus EQ (7) can be written as $\tau_{\mathrm{eff}} \approx \tau_{\mathrm{c}}$. The confined fast tritons are considered to be due to increase with n_{e}. Therefore, triton burnup ratio increases with n_{e} in the low-n_{e} phase. When density reaches to around $2.5 \times 10^{19}\ \mathrm{m}^{-3}$, the slowing-down time is too short, and EQ (7) can be written to $\tau_{\mathrm{eff}} \approx \tau_{\mathrm{se}}$. Short τ_{eff} means low triton confinement. This is due to energy loss being too fast, thus the energy of triton becomes lower than 170 keV (peak cross section), where the reactivity of D-T is very low. Therefore, triton burnup ratio decreases with decrease of τ_{se} in high-n_{e} phase as shown in Fig. 2 and Fig. 3.

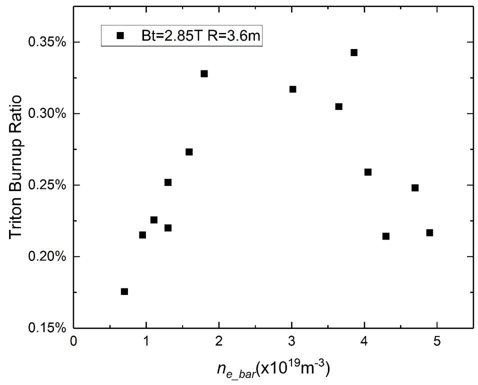

Fig. 2 Line-averaged density dependence of triton burnup ratio in same magnetic field strength and magnetic axis position.

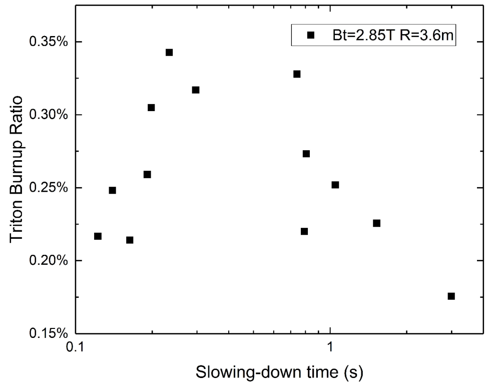

Fig. 3 The slowing-down time dependence of triton burnup ratio.

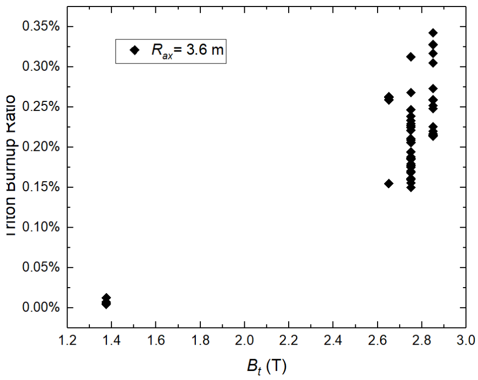

Fig. 4 Magnetic field dependence of triton burnup ratio.

Figure 4 shows that triton burnup ratio strongly depended on magnetic field B_t. When B_t decreased to one-half of 2.75 T, triton burnup ratio was almost close to 0. Collisionless orbits of helically trapped energetic ions in magnetic axis (R_{ax}) of 3.6 m, 3.75 m, and 3.9 m are shown in Fig. 5. The drift surface of trapped energetic ion in R_{ax} of 3.6 m matches with magnetic flux surfaces relatively, which tends to deviate largely from magnetic flux surfaces as magnetic axis position is shifted outward [17]. The confinement property of helically trapped energetic ions largely depends on magnetic field configurations. The triton burnup ratios in R_{ax} from 3.6 m to 3.9 m are plotted in Fig. 6. The triton burnup ratio decreases as the plasma column shifts outwardly as expected from orbit calculations found in Fig. 6 in which the high triton burnup ratio is obtained in inwardly shifted configuration (R_{ax}/B_t = 3.6 m/2.75 T).

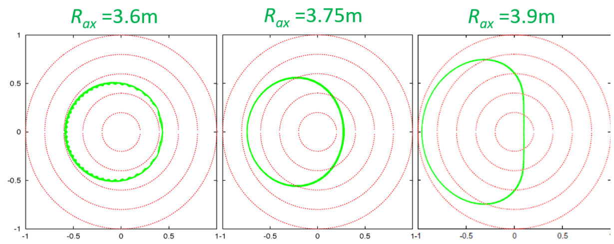

Fig. 5 Collisionless orbits of helically trapped energetic ions in R_{ax} of 3.6 m, 3.75 m, and 3.9 m.

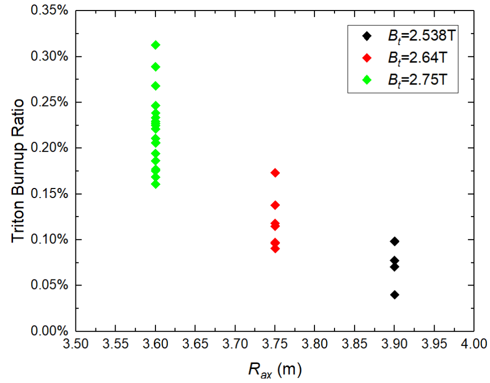

Fig. 6 The triton burnup ratios in different magnetic axis positions R_{ax}.

4. Time Evolution of Triton Burnup

The time evolution of 14 MeV neutrons from secondary D-T reaction has been measured by Sci.-Fi. detector. Shot-integrated 14 MeV neutrons yield measured by Sci.-Fi. detector was calibrated by NAS measurement. Tritons need time to slow down to cause secondary D-T reactions. The rise of D-T neutrons is much slower than that of D-D neutrons just after NBIs are injected as shown in Fig. 7. The slowing down time τ_{se} for 1 MeV triton was calculated to be 300 ms by EQ (5). The cross-section of D(t,n)He reaction have a peak around 170 keV in triton energy. The slowing down form 1 MeV to 170 keV needs 1.8 τ_{se}. Tritons are accumulated in the plasma according to the function of $\{1\text{-exp}(-t/\tau_{se})\}$. The time of 90% of the saturated triton population is estimated by approximately 2.3 τ_{se}. The rise time D-T neutron emission rate is the convolution of the effect of the D(t,n)He reaction peak and the triton accumulation. However, it can be estimated roughly by 1.8 τ_{se} + 2.3 τ_{se} = 5.1 τ_{se} ($\sim$ 1.5 sec), which is almost

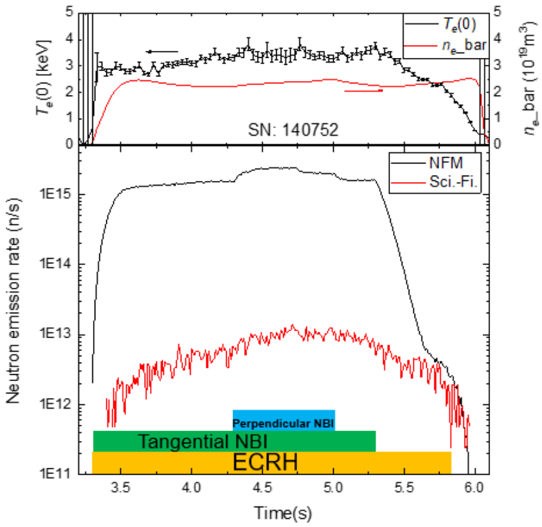

Fig. 7 Comparison of time evolution of D-T neutron measured by Sci.Fi. detector and total neutrons measured by NFM.

consistent with the rise time D-T neutron emission rate shown in Fig. 7. After the NBI turn-off, two decay time constants have been also observed from NFM data. The faster decay time (66.3 ms) corresponds to the D-D neutrons, and the slower decay time (333 ms) corresponds to D-T neutrons which have been confirmed by Sci.-Fi. detector data.

5. Conclusion

NAS has been utilized to perform cross checking of the absolute total neutron yield measured by NFM. The neutron yield evaluated by NAS is consistent with that measured with NFM. Most relative deviations between the NAS and NFM are less than 10%. This is the first time to measure 14 MeV neutrons on stellarators in the world. Triton burnup ratios are obtained to be 0 ~ 0.34% by the NAS measurement in this campaign. The triton burnup ratio increases with $\overline{n_e}$ below about 2.5×10^{19} m^{-3}, and decreases above that density. The triton burnup ratio decreases as the magnetic axis position shifts outward. The triton burnup ratio strongly depends on B_t. Time evolution of triton burnup data has been obtained, and calculation of the time evolution for triton burnup study will be carried out by using a classical slowing-down model.

Acknowledgments

This work was supported by the LHD project budgets (ULGG801, ULHH003, and ULHH034). This work was partly performed with the support and under the auspices of the NIFS Collaboration Research program (KOAH033). This work was also supported by the JSPS-NRF-NSFC A3 Foresight Program on critical physics issues specific to steady-state sustainment of high-performance plasmas in the field of Plasma Physics (NSFC: No. 11261140328, and NRF: No. 2012K2A2A6000443).

[1] A. Iiyoshi *et al.*, Nucl. Fusion **39**, 1245 (1999).
[2] M. Isobe *et al.*, Rev. Sci. Instrum. **85**, 11E114 (2014).
[3] N. Pu *et al.*, Rev. Sci. Instrum. **88**, 113302 (2017).
[4] M. Isobe *et al.*, Rev. Sci. Instrum. **81**, 10D310 (2010).
[5] L.C. Johnson *et al.*, Rev. Sci. Instrum. **66**, 894 (1995).
[6] C.W. Barnes *et al.*, Rev. Sci. Instrum. **61**, 3190 (1990).
[7] C.W. Barnes *et al.*, Nucl. Fusion **38**, 597 (1998).
[8] S. Conroy *et al.*, Nucl. Fusion **28**, 2127 (1988).
[9] M. Hoek *et al.*, "Triton burnup measurements at ASDEX Upgrade by neutron foil activation", IPP-Report IPP-1/320 (1999).
[10] M. Hoek *et al.*, Nucl. Instrum. Methods Phys. Res. A **368**, 804 (1996).
[11] H.H. Duong and W.W. Heidbrink, Nucl. Fusion **33**, 211 (1993).
[12] P. Batistoni *et al.*, Nucl. Fusion **27**, 1040 (1987).
[13] W.W. Heidbrink, R.E. Chrien and J.D. Strachan, Nucl. Fusion **23**, 917 (1983).
[14] J. Jo *et al.*, Rev. Sci. Instrum. **87**, 11D828 (2016).
[15] N. Pu *et al.*, Rev. Sci. Instrum. **89**, 10I105 (2018).
[16] T.H. Stix, Plasma Phys. **14**, 367 (1972).
[17] S. Murakami *et al.*, J. Plasma Fusion Res. SERIES **5**, 620 (2002).